The manuscript is currently under consideration in the *Bulletin of Engineering Geology and the Environment*.

Title: Influence of temperature on the residual shear strength of landslide soil: role of the clay fraction

Authors: Om Prasad Dhakal (1), Marco Loche (1,2), Ranjan Kumar Dahal (3), Gianvito Scaringi (1,*)

Affiliations:
(1) Institute of Hydrogeology Engineering Geology and Applied Geophysics, Charles University, Albertov 6, Prague, 128 43, Czech Republic.
(2) Institute of Rock Structure & Mechanics, Czech Academy of Sciences, V Holesovickach 41, Prague, 182 09, Czech Republic.
(3) Central Department of Geology, Tribhuvan University, Kirtipur, Kathmandu, 44600, Nepal.

(*) Corresponding author. E-mail: gianvito.scaringi@natur.cuni.cz;

Influence of temperature on the residual shear strength of landslide soil: role of the clay fraction

Om Prasad Dhakal[1], Marco Loche[1,2], Ranjan Kumar Dahal[3] and Gianvito Scaringi[1*]

[1]Institute of Hydrogeology, Engineering Geology and Applied Geophysics, Charles University, Albertov 6, Prague, 128 43, Czech Republic.

[2]Institute of Rock Structure & Mechanics, Czech Academy of Sciences, V Holešovičkách 41, Prague, 182 09, Czech Republic.

[3]Central Department of Geology, Tribhuvan University, Kirtipur, Kathmandu, 44600, Nepal.

*Corresponding author(s). E-mail(s): gianvito.scaringi@natur.cuni.cz;
Contributing authors: dhakalo@natur.cuni.cz; marco.loche@natur.cuni.cz; ranjan.dahal@cdgl.tu.edu.np;

Abstract

The shear strength is a fundamental parameter of soil that controls the occurrence and propagation of landslides. In pure clays, it depends on temperature according to the mineralogy, stress history, and hydro-mechanical boundary conditions. Landslide soils, however, are typically very heterogeneous and have a variable content of fines. The sensitivity of the residual shear strength of low-plasticity soil to temperature, in particular, is poorly understood, leaving significant uncertainties on the potential role of thermal forcing in landslides. We conducted ring-shear experiments on remoulded low-plasticity soil samples from the Melamchi catchment in central Nepal, where a large disaster occurred in 2021, with fifteen simultaneous landslides along the river corridor and a destructive flood. We performed the experiments in water-saturated conditions under representative normal stress values (50-100-150 kPa) and a constant rate of shearing (0.1 mm/min).

During each test, we controlled the temperature and performed a heating-cooling cycle (20-50-20°C) with the shearing ongoing. To evaluate the role of the clay fraction (grain size <0.002 mm), we obtained specimens from the same soil samples by retaining the finest portion under three different cutoff grain sizes (0.125, 0.063, and 0.020 mm). The collected data were analysed statistically, using variance and skewness to evaluate the goodness of interpretation. A t-test was also implemented to exclude data close to the experimental uncertainty, delineating the experiment's significance at a 68% confidence interval ($1\boldsymbol{\sigma}$). Our results revealed a decreased residual shear strength upon heating (thermal weakening), with the magnitude of this weakening correlating with the specimen's clay fraction and normal stress. Notably, a response to heating only emerged in specimens with a clay fraction of at least 10% and higher clay fraction and normal stress were conducive to greater weakening. Yet, the observed effect was relatively small, corresponding to a decrease in friction angle of just ∼1°. This suggests a minor role of temperature in the response of sheared low-plasticity soil; however, more experiments are needed, covering the wide range of mineral compositions of clayey soils, to understand the role of temperature in the shearing process and formulate robust empirical laws to quantify thermal effects.

Keywords: Residual shear strength, thermo-mechanical coupling, temperature, slope stability, landslide, clay

1 Introduction

The shear strength of soil plays a key role in many aspects of civil and structural analysis. It is defined as the capacity of soil to resist deformation under applied shear forces [1–3], and is assessed, contextually, in terms of the peak, critical, and residual shear strengths of specimens in the laboratory [4, 5]. In landslide research, the peak and fully softened strength, also known as the critical strength, are considered to govern the instability of a newly developed slope failure [6]. In contrast, the residual shear strength is generally understood as the resistance to be mobilised to reactivate a previously displaced failure plane, such as a bedding shear or fault zone [3, 4, 7, 8]. Specifically, the drained residual shear strength is crucial in evaluating the long-term stability of slopes [7, 9].

The experimentally measured soil strength is influenced by several factors, which are either related to the material (mineral composition, grain shape and size, pore fluid chemistry) or the test design (normal stress, shear rate, laboratory temperature) [10–14]. Coupling among these factors is not straightforward, yet a major role of mineralogy has emerged in past research [15–17]. For instance, Tiwari [15] proposed a triangular model to estimate the residual shear strength according to the proportion of three mineral groups (smectite, kaolinite, and quartz/feldspar). Dependencies were also established with respect to index properties [3, 7, 18, 19] and grain shape [7, 19]. Finally, the shear strength also depends on ion concentrations in the pore fluid [17, 20, 21]. Regarding the test design, the normal stress has a strong relationship with the shear strength, while the role of the rate of shearing is still a matter of research [10, 19, 22–24]. In general, attempts to correlate the residual shear strength to the rate of shearing pointed out that ”rate effects” tend to become significant above a threshold rate in the range of 0.1-1.0 mm/min in usual testing equipment [22, 25], corresponding to a strain rate in the order of 0.01 s^{-1}.

Research on thermal effects on the mechanical strength of soil was initiated in the 1960's, yet the dependencies are, to date, unclear. Mitchell [26] suggested no substantial difference in soil strength for temperatures ranging between 10 and 60 °C, with subsequent experiments confirming this observation [27–29]. However, the growing interest in clay barriers for radioactive waste disposal [30] and the complex interactions between soil and energy piles [31] prompted improvements in experimental devices and designs in recent decades [32]. Studies thus demonstrated a variety of behaviours according to temperature and stress-thermal histories, such as enhanced consolidation [33, 34] and hydraulic conductivity associated with a reduced pore water viscosity at elevated temperature [35]. Loss of pore fluid due to heating may cause a collapse of high-porosity clay structures, resulting in macroscopic settlements. Various researchers pointed out the major role of the volumetric response of soils upon heating or cooling compared to their shear response, resulting in a somewhat reduced research interest towards the latter [16, 36–43].

Recently, however, an interest towards achieving a comprehensive understanding of the role of climatic forcing and climate change in the stability of slopes and landslide dynamics [11, 24] justified experimental campaigns whereby direct or ring-shear experiments were conducted, aimed at evaluating the thermal sensitivity of the residual shear strength, particularly in soils containing clay minerals [13, 14, 44]. Evaluations centred on clays, as landslide shear zones often contain clay minerals also owing to mechanical breakage and weathering processes. More in general, the clay fraction has a strong control on the stability of soil masses, as clays are the most sensitive soil components to changes in boundary conditions, producing macroscopic volumetric and strength changes as well as long-term time-dependent responses [45–47]. Case studies [44, 48] showed that a cooling-induced weakening could explain a number of landslide remobilisations unrelated to precipitation or snowmelt in smectite-rich soils. Similar experiments pointed out the high thermal sensitivity of high-plasticity clays [13, 14]. However, quantifying this sensitivity is not straightforward as smectite strengthens upon heating under very slow shearing, whereas it weakens under faster shearing [13, 14, 48]. Overall, clay soils exhibit either thermal strengthening or weakening according to their mineral composition and rate of shearing [14]. Yet, the conclusion is limited because of the difficulty in evaluating changes in pore water pressure in the shear zone during fast shearing [12].

In contrast, research falls short in showing the thermal sensitivity of low-plasticity soils, abundant in mountain environments that are especially susceptible to global warming [49]. Recent experiments demonstrate that as sand is added to clay soil, thereby reducing its clay fraction and plasticity, its thermal sensitivity decreases and vanishes; however, some other experiments show that sand-clay mixtures or natural clay soils may exhibit higher thermal sensitivities than pure smectites [13, 44, 48].

Here, we will discuss the results of temperature-controlled ring-shear experiments conducted on specimens of natural soil under a low rate of shearing. In particular, we will focus on low-plasticity soils from a recent landslide-related disaster in Nepal to contribute to the evaluation of possible thermo-mechanical conditioning on slope stability, an understudied matter that is becoming increasingly relevant in the context of global warming [11, 50]. In our study, we aim to better understand the role of the clay fraction in controlling the thermal sensitivity of the residual shear strength and identify a possible threshold (% clay fraction) below which thermal effects could be ruled out. Also, we propose that the observed thermal sensitivity could be linearly correlated with the clay fraction, as this may simplify the upscaling of laboratory insights to a coarser spatial coverage.

2 Materials and methods

The methodological workflow within this research comprises the preparation of specimens for the ring-shear tests to showcase a spectrum of responses relating to the materials' clay fraction. Each specimen is sheared in a modified ring-shear device that can allow for controlled temperature variations during shearing. All the experiments are conducted with a consistent test design to ensure data consistency. Finally, a statistical approach for data analysis is implemented so as to quantify the observed effect with a certainty factor. Each aspect is explained below under separate headings.

2.1 Sample properties and preparation

The materials were sampled in the Melamchi catchment in Nepal, which experienced a large catchment-scale disaster in 2021 [51–53]. The trigger of the disaster was an outbreak of a small glacial lake accompanied by precipitation and entrained valley walls, resulting in an enormous debris flood downstream. This trigger may be correlated with the warming of the region as studies show the area may become up to 4.9°C warmer by 2100 [54] in a worst-case scenario (RCP 8.5). The post-disaster survey included sampling at 70 locations, including landslide scarps, old landslide deposits, and areas affected by landslide runout. At each location, the sample was collected to a depth of 1 m using a manual auger to penetrate the topsoil layer.

We selected four samples for our investigation, which were transported to the soil mechanics laboratory in Czechia in sealed containers in the frame of a collaboration between our institutions and between our national groups of the IAEG. These four samples (Figure 1), chosen based on mineralogical differences, were further processed to produce 12 specimens with distinct grain size distributions, as shown in Figure 2. The preparation of three specimens out of each of the four soil samples was achieved via wet-sieving using ISO3310-2 [55]-compliant sieves retaining grain sizes of <20, <62, and <125 μm. We did not use dry sieving owing to the difficulty of separating the finest fraction in the absence of water. Further, for each grain size cutoff, the percentage clay fraction was calculated by the ratio of clay available within the sample to the respective amount of coarse fragments retained by the three sieves. The total available clay was calculated from the grain size chart (obtained with hydrometer analysis) corresponding to the grain diameter of 0.2 μm. Details of each specimen are shown in Figure 2.

Fig. 1 The four soil samples tested in this work after pre-sieving through the 425μm sieve.

Sample	Natural moisture content (w%)	Bulk density (gm/cc)	Dry density (gm/cc)	Cohesion (kPa)	Friction angle (°)	Liquid limit (%)
A68	8.9	1.3	1.2	11.6	27.4	36
A71	9.0	1.6	1.5	6.9	29.2	23
A69	7.5	1.3	1.2	13.6	30.1	35
A31	32.0	1.5	1.1	14.0	32.0	23

Table 1 Properties of the four soil samples used in this study evaluated in the experimental campaign conducted in Nepal [56].

X-ray Powder Diffraction (XRD) analysis [57] was carried out to obtain the semi-quantitative mineralogical composition of the samples, as shown in Table 2. The experiments were performed using an X-ray diffractometer (X'Pert Pro), and the data were analysed using the X'Pert Highscore™ data analysis software version 1.0d (PANalytical, Almelo, The Netherlands). The machine setting was as follows: anode target of copper, acceleration voltage of 40 kV generating 30 mA of electric current. Continuous scanning was done from 3 to 60°2θ with a step size of 0.05 °2θ scanning for 200 s on each time step. Table 2 shows the mineralogical composition of the tested samples. The experiments showed that most samples contained quartz, plagioclase, and muscovite.

Notably, discerning the various clay minerals proved to be challenging owing to their small proportion.

Sample	A69	A71	A31	A68
Quartz	59	36	64	57
Plagioclase	16	11	15	19
Chlorite	4		3	4
Gibbsite			6	5
Microcline		3	5	6
Muscovite	4	20	3	4
Kaolinite	3	5	3	4
Silimanite		25		
Ankerite				1
Orthoclase	10			
Amphibole	4			

Table 2 Semi-quantitative(%) mineralogical composition of the tested soil samples according to X-ray powder diffraction analysis.

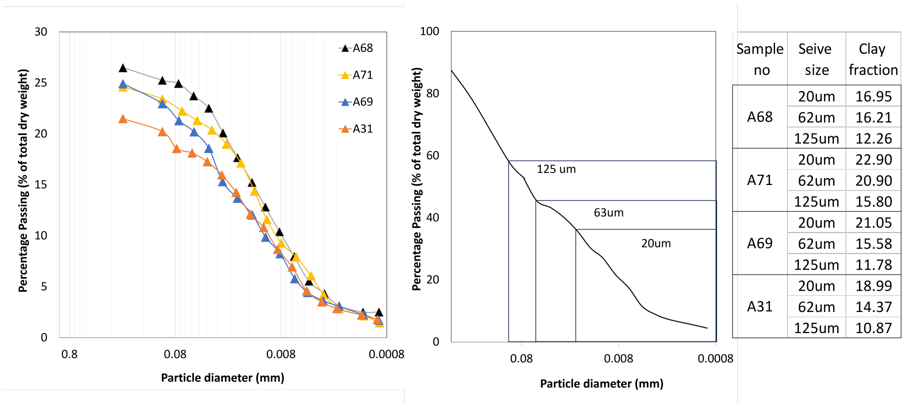

Fig. 2 Left to right: grain size curves (in log-scale) of the samples tested, schematic representation of the extraction of specimens with various clay fractions from the four samples

2.2 Ring-shear setup with temperature control

A commercial Bromhead-type ring-shear device was utilised for the experiments [2]. Specifically, a Torshear EmS [58], produced under Wykeham Farrance and manufactured by Controls, was modified to enable temperature control (Figure 3), following Loche and Scaringi [14]. The ring-shear apparatus complies with the ASTM 6467 standard [59].

The device has a rotating base plate lined with a roughened porous platen. The box accommodating the material has an annular shape with a thickness of 5 mm and a width of 30 mm (100 mm outer diameter, 70 mm inner diameter), thus featuring an area of 40 cm^2. Normal and shear stresses are transferred through a rotating top cap lined with a roughened porous platen

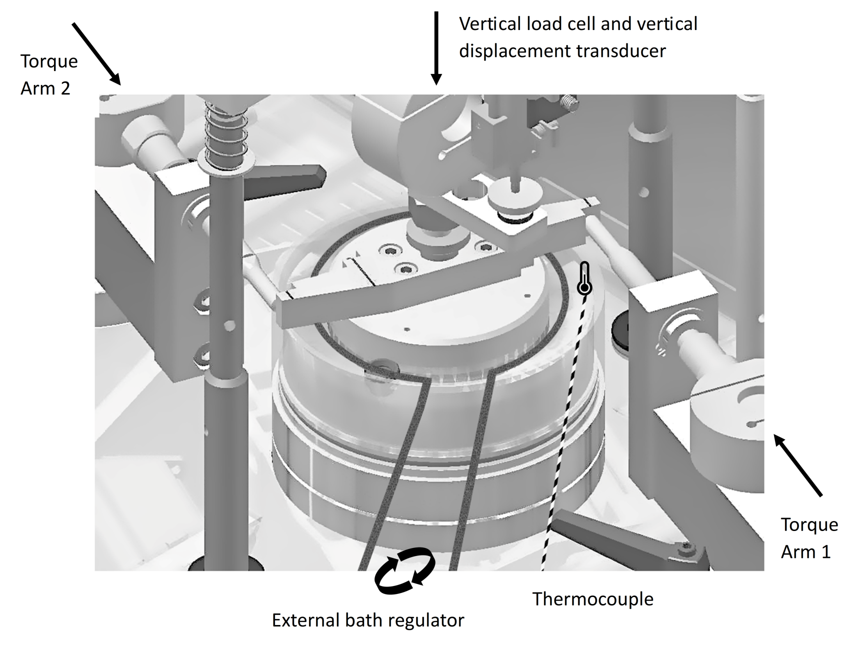

Fig. 3 Schematic of the ring-shear apparatus showing the placement of the external temperature control circuit and thermocouple.

to enhance drainage and avoid interface shearing. Two orthogonal torque arms are connected to stiff load cells to measure the shear resistance arising from the soil rotation. The shear strength was calculated using a standard procedure according to the ASTM D6467-13 [59].

Temperature control is achieved through an external thermostatic bath that provides a water flow at a controlled temperature in a closed circuit consisting of a pipe of conductive material partly submerged in the device's water bath. Owing to heat losses in the circuit, which cannot be perfectly insulated, the temperature associated with the testing is measured within the water bath. We know that a delay exists between changes in temperature in the bath and within the soil, mainly associated with the time for heat transfer through the porous platens (made of brass, an excellent heat conductor).

A pump ensures water flow in the circuit, and sufficient thermal inertia is guaranteed by a 3-litre thermostatic bath equipped with an electric heater. Due to inevitable losses in the system, in order to maintain a constant temperature of 50°C in the ring-shear's water bath, a higher temperature is set in the thermostatic bath. Pre-heated distilled water is manually added in both baths as needed to keep the water levels constant without causing disturbances in the experiment.

2.3 Experimental design and data analysis

To enable comparisons, the 12 specimens with different clay fractions (Figure 2) were tested in identical conditions. In particular, three normal stresses (50, 100 and 150 kPa) were used to evaluate the specimens' Mohr-Coulomb failure criterion. A total of 36 experiments were conducted, as summarised in Table 3. The shearing rate was set to 0.1 mm/min, which was deemed sufficiently low for significant shear-rate effects to arise, owing to the soils' low plasticity (<23%) [60], and sufficiently fast to ensure sufficient shear displacements during the heating-cooling phases, which had to be performed under human supervision.

Before the shearing phase, the specimens were consolidated in the ring-shear device under a normal stress of 600 kPa. Step-wise loading was performed, and the consolidation curves were monitored to ensure the dissipation of the pore water pressure excess prior to further loading. Step-wise unloading was then performed to the desired normal stress. The specimens were overconsolidated to enhance their structural anisotropy, to favour a preferential alignment of the clay particles in the direction orthogonal to the applied stress (and parallel to the shearing direction), thus facilitating the subsequent shearing phase. Overconsolidation also enhanced the specimens' normal stiffness, reducing secondary volume changes in the soil portion not directly affected by the shearing.

The specimens were sheared until the residual shear strength was attained, that is, until a steady value of shear resistance was recorded after large shear displacements. The specimens were sheared further in the residual condition for at least 10 mm (∼2 h) at room temperature (20°C); then, the temperature of the water bath was progressively increased to 50°C using the external thermostatic bath. To aid the interpretation of the experiments, we identified five stages (Figure 4), described as follows. The residual shear strength of the soil at 20°C was observed in stage 1. In stage 2, after some further shearing, the soil undergoes rather rapid heating, leading to a transient response that cannot be assessed owing to the absence of pore water pressure measurement. The duration of this transient response should be closely related to the hydraulic conductivity of the soil, but is also influenced by the stiffness of the soil portion beneath the shear zone, which remains overconsolidated. Difficulties in assessing this transient response have been pointed out in the literature [14, 44]. During the heating phase (Figure 4, stage 2 and 3), the temperature of the water bath is increased and then kept constant until a new steady value of the shear resistance is observed over a distance of at least 10 mm (stage 3). By the end of this stage, we assume that the soil has reached a new equilibrium with the boundary conditions and, in particular, that pore water pressure excess has dissipated, primary consolidation is completed, and thermally-induced volume changes have occurred. In stage 4, the experimental setup is set to cool down naturally to room temperature (20±1°C). After the weakening observed in stage 3, complete strength recovery is usually observed in stage 4. This recovery occurs over a longer period of time, but it seems synchronous with respect to the cooling. In stage 5, we continue shearing at room temperature to confirm the reversibility of the effects of the heating-cooling cycle.

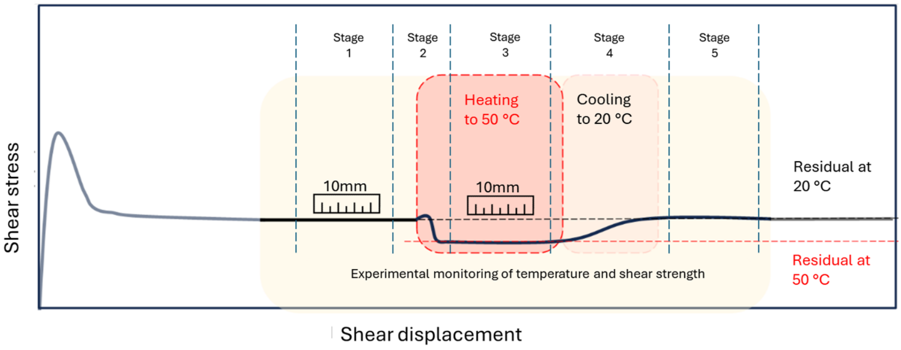

Fig. 4 Typical output of a ring-shear experiment featuring a heating-cooling cycle, in terms of shear stress vs. shear displacement. A description of the stages (1-5) is provided in the text. The 10-mm bars show the intervals of data extraction from the experiment for the statistical test.

2.4 Statistical analysis

Considering the uncertainties arising from the characteristics of the experimental device, the sensors for data acquisition, and the variability of the shear response itself, we opted for a statistical framework to analyse a large number of experimental data and evaluate less subjective values of shear strength. An equal number of data points (300 each) of measured shear resistance from stages 1 and 3 (Figure 4) were extracted to observe the data quality by plotting the variance and skewness of the data. Individual test results (expressed as shear resistance divided by the normal stress) and their probability density function (PDF) are shown in Figures 5 and 6. The mean of the 300 points each at stages 1 and 3 are considered the residual friction coefficient at 20°C and 50°C, respectively. The values are also presented in Table 3. Overall, the data variance was more pronounced in the experiments conducted under lower normal stress on specimens with lower clay fraction, whereas the experiments conducted under the highest normal stress and with the largest amount of fines showed the tallest and most distinctly separated distributions.

To provide a further way to discuss the thermal effect quantitatively, we verified whether the temperature change produced a variation in the residual shear strength of >1 kPa, labelling as "no effect" any observed variation below this threshold. We chose this value as a threshold for significance as it lies close to the experimental device's error range. We used Welch's t-test, where we took, as the null hypothesis, the statement that the true difference between the residual friction coefficient evaluated at 50°C and that evaluated at 20°C is <1 kPa. The sampling size was the same as that used for the calculation of the residual shear strength (i.e. 300 points for each set), and we opted for a 68%

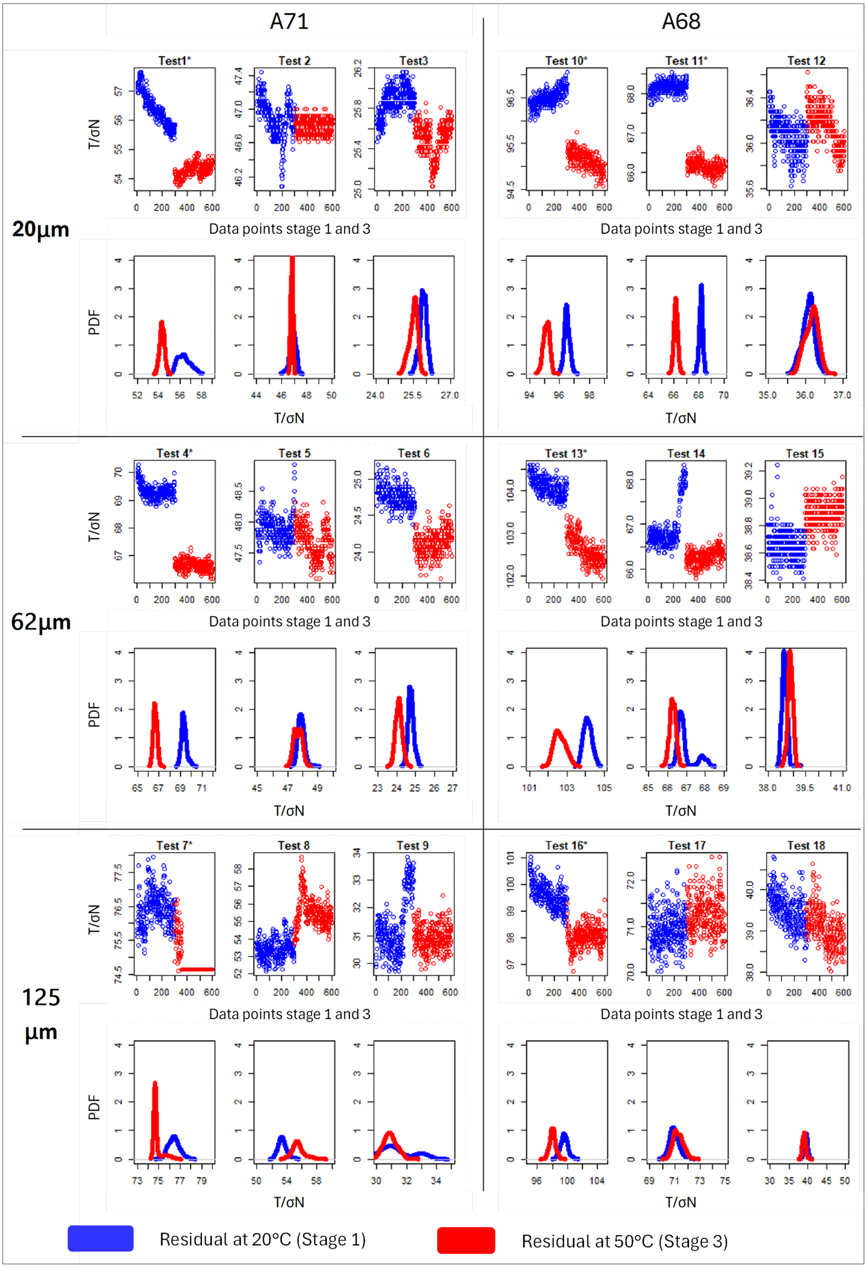

Fig. 5 Strength measurement extracted from stages 1 and 3 complemented by a probability density function (PDF) of the data scatter. The plots refer to the tests performed on soil samples A71 (left) and A68 (right). The symbol (*) indicates statistically significant tests.

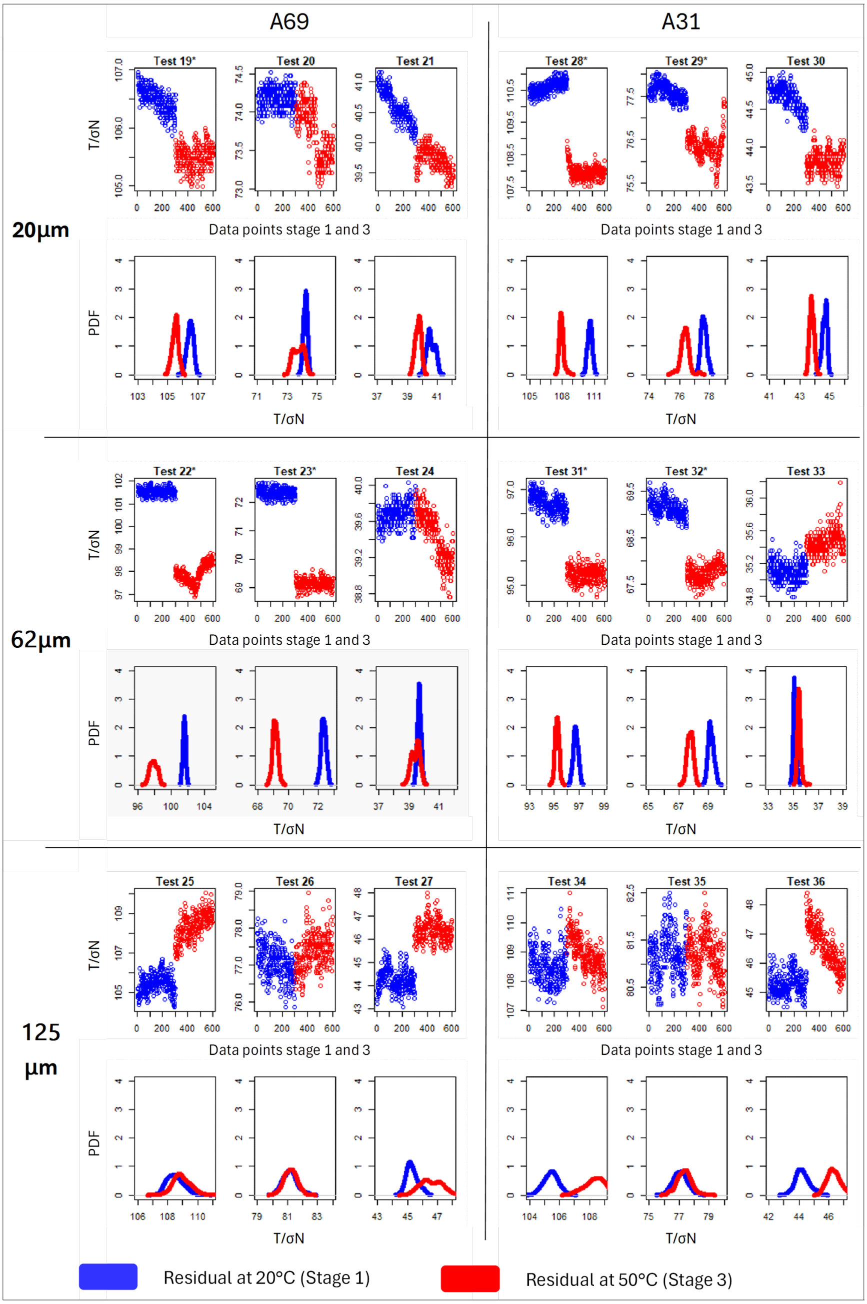

Fig. 6 Strength measurement extracted from stages 1 and 3 complemented by a probability density function (PDF) of the data scatter. The plots refer to the tests performed on soil samples A69 (left) and A31 (right). The symbol (*) indicates statistically significant tests.

confidence interval (±1 standard deviation) The t-test results are reported in Table 3.

3 Results and Discussion

Table 3 Summary of results of the temperature-controlled ring-shear tests.

Sample	Grain size cutoff (μm)	Test no.	Normal stress (σ, kPa)	Residual shear strength at 20°C (τ_{r0}, kPa)	Residual shear strength at 50°C (τ_{r1}, kPa)	Residual friction coefficient at 20°C (τ_{r0} / σ)	Residual friction coefficient at 50°C (τ_{r1} / σ)	Variation in residual friction coefficient ($\Delta\tau_r$ / σ)	Variation in residual friction coefficient per 1°C ($\Delta\tau$ / ΔT∗100)	t-test for a 68% confidence interval (significance: $p >$ 0.32)	Thermal effect
		1	150	56.37	54.31	0.376	0.362	-0.014	-0.046	Yes	Weakening
	20	2	100	46.89	46.81	0.469	0.468	-0.001	-0.003	No	No effect
		3	50	25.88	25.49	0.518	0.510	-0.008	-0.026	No	No effect
		4	150	69.32	66.65	0.462	0.444	-0.018	-0.059	Yes	Weakening
A71	63	5	100	47.89	47.68	0.479	0.477	-0.002	-0.007	No	No effect
		6	50	24.76	24.11	0.495	0.482	-0.013	-0.043	No	No effect
		7	150	76.43	74.83	0.510	0.499	-0.011	-0.036	Yes	Weakening
	125	8	100	53.40	55.52	0.534	0.555	0.021	0.071	No	No effect
		9	50	31.40	30.91	0.628	0.618	-0.010	-0.033	No	No effect
		10	150	96.50	95.13	0.643	0.634	-0.009	-0.030	Yes	Weakening
	20	11	100	68.17	66.15	0.682	0.662	-0.020	-0.067	Yes	Weakening
		12	50	36.06	36.15	0.721	0.723	0.002	0.006	No	No effect
		13	150	104.10	102.62	0.694	0.684	-0.010	-0.033	Yes	Weakening
A68	63	14	100	66.93	66.28	0.669	0.663	-0.006	-0.022	No	No effect
		15	50	38.82	38.90	0.776	0.778	0.001	0.005	No	No effect
		16	150	99.59	98.04	0.664	0.654	-0.010	-0.035	Yes	Weakening
	125	17	100	70.94	71.26	0.709	0.713	0.003	0.011	No	No effect
		18	50	39.50	39.06	0.790	0.781	-0.009	-0.029	No	No effect
		19	150	106.49	105.50	0.710	0.703	-0.007	-0.022	Yes	Weakening
	20	20	100	74.19	73.73	0.742	0.737	-0.005	-0.015	No	No effect
		21	50	40.59	39.72	0.812	0.794	-0.017	-0.057	No	No effect
		22	150	101.55	97.90	0.677	0.653	-0.024	-0.081	Yes	No effect
A69	63	23	100	72.33	69.13	0.723	0.691	-0.032	-0.107	Yes	Weakening
		24	50	39.68	39.44	0.794	0.789	-0.005	-0.016	No	No effect
		25	150	108.48	108.93	0.723	0.726	0.003	0.010	No	No effect
	125	26	100	81.15	81.19	0.812	0.812	0.000	0.001	No	No effect
		27	50	45.30	46.58	0.906	0.932	0.026	0.085	No	No effect
		28	150	110.61	107.96	0.737	0.720	-0.018	-0.059	Yes	Weakening
	20	29	100	77.60	76.35	0.776	0.763	-0.013	-0.042	Yes	Weakening
		30	50	44.65	43.81	0.893	0.876	-0.017	-0.057	No	No effect
		31	150	96.71	95.21	0.645	0.635	-0.010	-0.033	Yes	Weakening
A31	63	32	100	69.15	67.75	0.691	0.678	-0.014	-0.046	Yes	Weakening
		33	50	35.11	35.46	0.702	0.709	0.007	0.023	No	No effect
		34	150	105.44	108.37	0.703	0.722	0.020	0.065	No	No effect
	125	35	100	77.07	77.34	0.771	0.773	0.003	0.009	No	No effect
		36	50	44.25	46.34	0.885	0.927	0.042	0.140	No	No effect

3.1 Temperature-induced variations in soil strength

Thirty-six temperature-controlled ring shear experiments were conducted, for which the measured residual shear strength values at 20°C and 50 °C are shown in Table 3. A summary of the tests in terms of the friction coefficient as a function of the shearing distance during the heating-cooling cycle is presented in Figure 7.

The dominant behaviour is that of a slight weakening upon heating, usually followed by full recovery after cool-down. However, a transient response is also observed (stage 2) in almost all the experiments, characterised by a spike of shear strengthening, likely due to the rapid heating. The spike is followed by a progressive decline to a steady value of shear strength, usually lower than what was measured at 20°C. The spike could be explained by the generation of a negative pore water pressure caused by thermal expansion. The phenomenon, however, is not of immediate understanding as the disparity between the much higher volumetric thermal expansion coefficient of water compared to that of the soil minerals ($2{-}5{\cdot}10^{-4}$ vs. $1{-}3{\cdot}10^{-5}$) should result in a positive pore water pressure excess. Experiences from the literature [61] highlight the important role of overconsolidation, whereby highly overconsolidated clays exhibit an expansive and recoverable response while normally consolidated clays exhibit a contractive and partially non-recoverable response. These are consistent with generating negative and positive pore water pressure excess, respectively. Thus, the magnitude of the spike should scale with the overconsolidation ratio and be largest at the lowest normal stress. Also, it should scale with the clay fraction and be the largest for the smallest cutoff grain size. However, this cannot be observed clearly in our experiments as the clay fraction tested is not substantially farther amongst tested specimens.

In addition, the observed transient response could also derive from a partially undrained condition resulting from rapid heating. In undrained conditions, however, the literature shows shear weakening upon heating in normally consolidated clays [61]. Our sheared specimens are heterogeneous owing to overconsolidation, featuring a normally consolidated shear zone on an underlying overconsolidated non-sheared layer. The shear and volumetric responses of the specimens may be attributable to the characteristics of these two layers. However, evaluating the thickness of the shear zone in a Bromhead-type apparatus is challenging as the overall thickness of the specimen at the end of the experiment is 3-4 mm at most, and a clear boundary between sheared and non-sheared materials cannot be discerned. Further, in explaining the observed spike, it should also be noted that heating does not occur homogeneously in the shear box. As the temperature in the water bath increases, heat transfer should proceed rapidly in the steel base and the brass porous platens, directed radially inwards. The soil should thus begin heating from the outer, top and bottom boundaries, with the shear zone (located at the top of the specimen) possibly heating faster, on average, than the underlying non-sheared layer. To sum up, the transient process could be further clarified through a heat transfer model coupled with a thermo-hydro-mechanical model. However, this goes

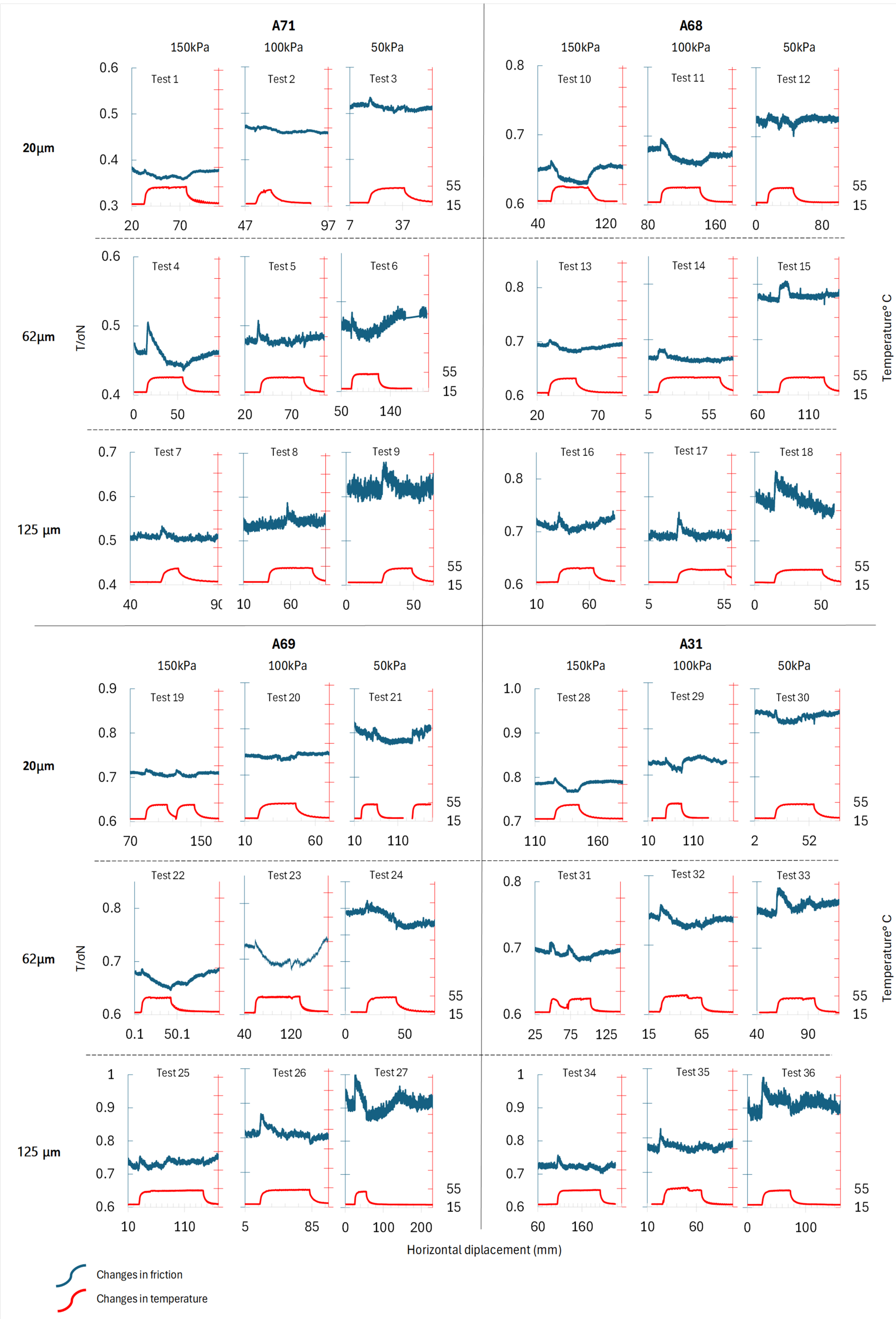

Fig. 7 Synoptic view of the observed changes in friction coefficient during the heating-cooling cycle performed in all 36 experiments.

beyond the scope of this work as we are not interested in the intermediate stage but in the steady-state value of shearing resistance at 50°C, corresponding to stage 3 in our experimental design.

Concerning this value (stage 3), we observed weakening to some extent, depending on the applied normal stress and the proportion of fines. In general, we observed a more significant effect of temperature under larger normal stress values, possibly associated with the better definition of the residual shear condition (particle alignment) that features more face-to-face contacts between particles, whose shearing behaviour is more governed by physicochemical forces than by the friction at face-to-edge or edge-to-edge contacts. When the soil heats, dilation alters the distance between the clay particles, and this alteration disrupts the equilibrium of physicochemical forces, resulting in a response of larger magnitude in the specimens tested with larger amounts of fines [33]. Furthermore, water viscosity is lower at elevated temperatures, promoting hydraulic flow and viscous deformations (both volumetric and in shear). The observed weakening is generally compatible with these micro-scale processes, and advanced modelling remains necessary to explain the observed response.

3.2 Effect of the grain size

Our experiments show that the effect of temperature is larger when fine particles are more abundant. This is expected in light of the above discussion and considering that in coarse-grained materials, a steady-state effect of temperature in the tested range, if any, should be attributed solely to a change in water viscosity. However, in coarse-grained materials subject to slow shearing, the free water in the pores should not affect the shearing process because water should flow freely without significant pore water pressure excess arising or significant interactions with the grains' surfaces. In fine-grained soils (or in the presence of a significant proportion of fines), a role of the adsorbed water should emerge, whereby the thermal expansion of the diffused double layer should be conducive to lower shearing resistance owing to the larger distance between clay particles in a face-to-face arrangement.

We present the results first in terms of the τ vs. σ plot as shown in Figure 8 where, according to the Mohr-Coulomb failure criterion, the slope of the dotted line is the internal friction angle of the soil. Upon careful observation, the value of the internal friction angle remains unchanged in the column on the right part of Figure 8, which shows results for the largest grain size cutoff for each soil sample. However, when the coarser fragments are filtered with finer sieves (finest 20 μm in the leftmost column in Figure 8), the temperature effect emerges with the reduced internal friction angle when heated. The magnitude of the change in the friction angle upon heating is seen in Figure 9, where the difference in the friction coefficient is plotted against the clay fraction present within individual specimens.

An interesting observation is foreseen as within our experiments we identify a threshold at about 10% of clay fraction, below which negligible thermal

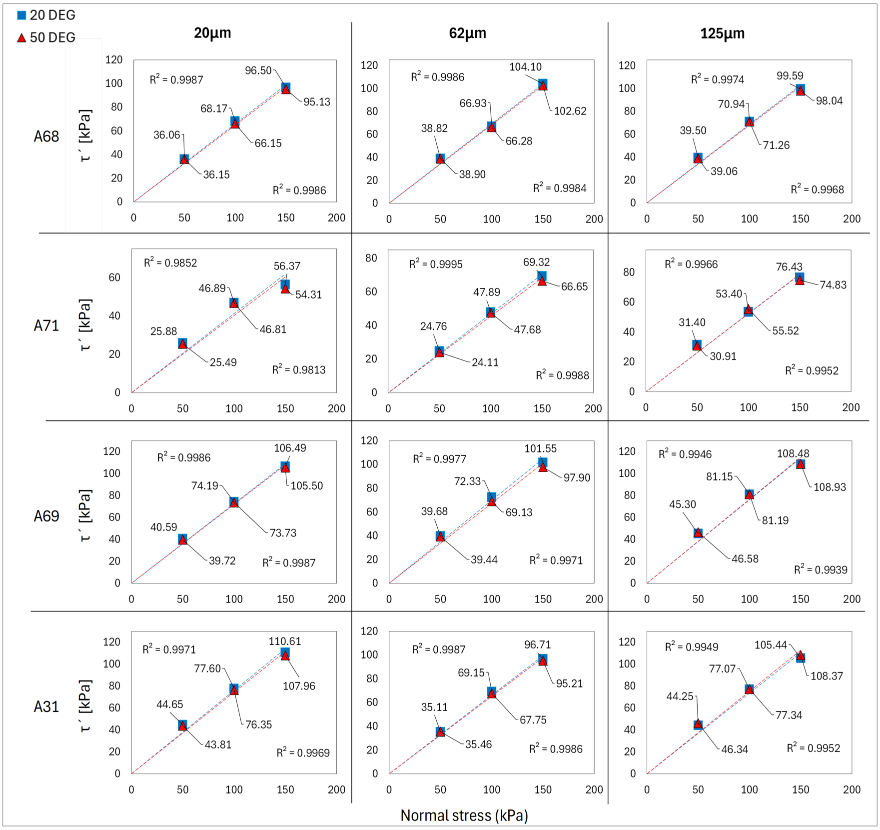

Fig. 8 Summary of the test results, expressed as residual shear strength values as a function of the normal stress. Mohr-Coulomb criteria for specimens tested at 20°C and 50°C are shown in the individual plots.

effects are observed, and above which the magnitude of the thermal effect seems to scale positively with the clay fraction (Figure 9). The identified threshold may vary according to the tested soil and, in particular, to the normal stress and the mineralogy of the clay component, as these affect the intergranular distances, coordination number, preferential orientation of grains, and the volumetric ratio of clay to non-clay minerals. In soils containing smectites, owing to the large water adsorption capacity of the latter and hence the high volumetric ratio (10% of smectite in dry weight can easily account for over 50% of the total soil volume when hydrated), we expect thermal effects to arise for even lower clay fractions, while we expect less response in soils containing bulky, less active clay minerals such as kaolinite [14]. As for the dependence of the magnitude of thermal effects on the clay fraction (above the threshold value), we note that this is consistent with the findings of Garcia et al. [13], who evaluated thermal effects in mixtures of bentonite and sand. The authors noted a large sensitivity of the thermal response to the presence of small amounts of smectite (up to 20%), with negligible further effects (i.e., small changes in the magnitude of the thermal effect) in soils with larger amounts of smectite (from 20% up to over 90%). However, important scattering was observed in the authors' interpretations, and none of the parameters considered (specific surface area, plasticity index, activity, smectite content, clay fraction) really stood out as the best proxy for predicting thermal effects. A similar situation was observed by Shibasaki et al. [44], but the smaller scattering in the authors' results allowed them to identify the smectite content as the best predictor.

Nonetheless, the definition of a threshold in terms of clay fraction could be useful to estimate — or exclude altogether — the effect of a changing temperature in the shear zone on the stability of preexisting landslide bodies. While natural soils are inherently heterogeneous, the clay fraction is commonly evaluated in sampled cores and can be retrieved from available maps for regional studies. Evaluations of clay mineralogy are less common but could yield more accurate estimations. Finally, the specialisation of the threshold by accounting for the effective normal stress (depth of the shear zone, pore water pressure regime) and the rate of shearing (remobilisation vs. acceleration of an ongoing movement) could be explored once sufficient experimental data become available.

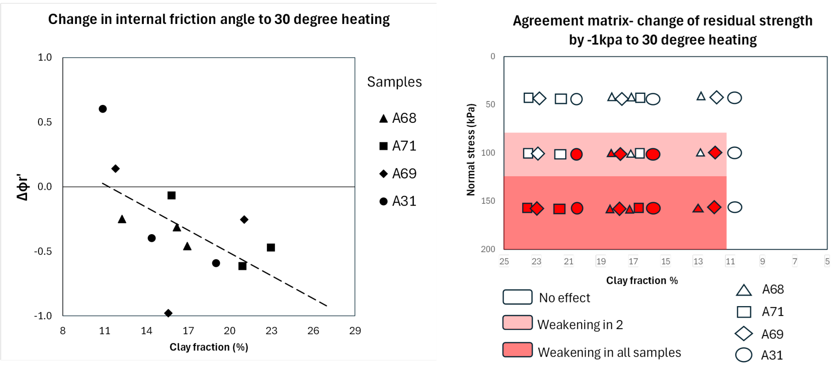

Fig. 9 Effect of temperature on the residual shear strength according to the clay fraction of the tested specimens. The left figure shows the difference in the internal friction angle to a 30°C heating. The right figure shows a matrix upon test conducted where temperature effect was prevalent, i.e reduction of 1 kPa of residual shear strength to a 30°C heating

4 Conclusions and Limitations

In this study, we investigated the influence of temperature on the experimentally determined residual shear strength of natural low-plasticity soils extracted from a landslide site in Nepal. The experiments were conducted at a low rate of shearing under various normal stress values. We explored, in particular, the role of the clay fraction and identified a threshold value (10%)

below which we were unable to evaluate a statistically significant response. Above the threshold, we observed lower strengths in samples tested at 50°C compared to those tested at 20°C (room temperature). Moreover, we found an increase in the magnitude of the thermal effect with the increase in clay fraction, both across the samples and by enriching the individual samples by excluding their coarse fraction according to different cutoff sizes. We are aware that the magnitude of the observed effect is minor, and its role may not be crucial in most landslide phenomena. Nonetheless, in refined analyses and in predictions of future instabilities, incorporating the thermal dimension and thermo-mechanical couplings may lead to performance improvements. As a matter of fact, the difference between the temperature in the field and that in the laboratory may introduce a systematic error in the laboratory determinations. Similarly, seasonal temperature oscillations in the shallow underground may cause variations in the available strength and, thus, in the factor of safety of slopes, which are typically unaccounted for. Ground warming caused by climate change via various processes (including heat transfer from the atmosphere, solar irradiation, but also changes in land use and deforestation) may alter the ground temperature in the long term. Again, accounting for a temperature-shear strength dependence could be beneficial in the predictive modelling of various types of landslide phenomena at the slope scale as well as at a wider catchment scale.

Acknowledgments. The authors acknowledge financial support from the Ministry of Education, Culture and Sport of the Czech Republic (MŠMT ERC CZ grant No. LL2316). O.P. Dhakal acknowledges support from the Charles University Grant Agency (GAUK grant No. 68624). The authors are also grateful to Tribhuvan University and Geotech Solutions International Pvt. Ltd. for providing samples and data from the study area.

Declarations

- Funding: See acknowledgement.
- Conflict of interest/Competing interests: The authors declare that there is no conflict of interest.
- Availability of data and materials: This work was built upon freely available datasets and tools.
- Code availability: Not applicable
- Authors' contributions:

Appendix A

References

[1] Bishop, A.W., Green, G., Garga, V.K., Andresen, A., Brown, J.: A new ring shear apparatus and its application to the measurement of residual strength. Geotechnique **21**(4), 273–328 (1971)

[2] Bromhead, E., Dixon, N.: The field residual strength of london clay and its correlation with loboratory measurements, especially ring shear tests. Géotechnique **36**(3), 449–452 (1986)

[3] Skempton, A.W.: Long term stability of clay slopes. Geotechnique **14**, 77–102 (1964). https://doi.org/10.1680/GEOT.1964.14.2.77

[4] Atkinson, J.: The Mechanics of Soils and Foundations, 2nd ed edn. Taylor and Francis, USA (2017)

[5] Mitchell, J.K., Soga, K., *et al.*: Fundamentals of Soil Behavior vol. 3. John Wiley and Sons New York, USA (2005)

[6] Stark, T.D., Choi, H., McCone, S.: Drained shear strength parameters for analysis of landslides. Journal of Geotechnical and Geoenvironmental Engineering **131**(5), 575–588 (2005)

[7] Lupini, J.F., Skinner, A.E., Vaughan, P.R.: The drained residual strength of cohesive soils. Géotechnique **31**, 181–213 (1981). https://doi.org/10.1680/geot.1981.31.2.181

[8] Stark, T.D., Eid, H.T.: Slope stability analyses in stiff fissured clays. Journal of Geotechnical and Geoenvironmental Engineering **123**(4), 335–343 (1997)

[9] Skempton, A.W.: Residual strength of clays in landslides, folded strata and the laboratory. Geotechnique **35**, 3–18 (1985)

[10] Scaringi, G., Hu, W., Xu, Q., Huang, R.: Shear-rate-dependent behavior of clayey bimaterial interfaces at landslide stress levels. Geophysical Research Letters **45**, 766–777 (2018). https://doi.org/10.1002/2017GL076214

[11] Scaringi, G., Loche, M.: A thermo-hydro-mechanical approach to soil slope stability under climate change. Geomorphology **401**, 108108 (2022). https://doi.org/10.1016/J.GEOMORPH.2022.108108

[12] Kohler, M., Hottiger, S., Puzrin, A.M.: Rate, water pressure, and temperature effects in landslide shear zones. Journal of Geophysical Research: Earth Surface **128**(9), 2023–007220 (2023)

[13] Garcia, L.M., Pinyol, N.M., Lloret, A., Soncco, E.A.: Influence of temperature on residual strength of clayey soils. Engineering Geology **323**, 107220 (2023). https://doi.org/10.1016/j.enggeo.2023.107220

[14] Loche, M., Scaringi, G.: Temperature and shear-rate effects in two pure clays: Possible implications for clay landslides. Results in Engineering **20**,

101647 (2023). https://doi.org/10.1016/J.RINENG.2023.101647

[15] Tiwari, B., Marui, H.: A new method for the correlation of residual shear strength of the soil with mineralogical composition. Journal of Geotechnical and Geoenvironmental Engineering **131**(9), 1139–1150 (2005)

[16] Maghsoodi, S., Cuisinier, O., Masrouri, F.: Thermal effects on mechanical behaviour of soil-structure interface. Can. Geotech. J **57**, 3247 (2020). https://doi.org/10.1139/cgj-2018-0583

[17] Moore, R.: The chemical and mineralogical controls upon the residual strength of pure and natural clays. Geotechnique **41**(1), 35–47 (1991)

[18] Stark, T.D., Eid, H.T.: Drained residual strength of cohesive soils. Journal of Geotechnical Engineering **120**, 856–871 (1994)

[19] Li, Y.R., Wen, B.P., Aydin, A., Ju, N.P.: Ring shear tests on slip zone soils of three giant landslides in the three gorges project area. Engineering Geology **154**, 106–115 (2013). https://doi.org/10.1016/j.enggeo.2012.12.015

[20] Bjerrum, L., Rosenqvist, I.T.: Some experiments with artificially sedimented clays. Géotechnique **6**(3), 124–136 (1956). https://doi.org/10.1680/geot.1956.6.3.124

[21] Di Maio, C., Santoli, L., Schiavone, P.: Volume change behaviour of clays: The influence of mineral composition, pore fluid composition and stress state. Mechanics of Materials **36**, 435–451 (2004). https://doi.org/10.1016/S0167-6636(03)00070-X

[22] Bhat, D., Yatabe, R., Bhandary, N.: Slow shearing rates' effect on residual strength of landslide soils. In: Soil Behavior and Geomechanics, pp. 293–303 (2014)

[23] Duque, J., Loche, M., Scaringi, G.: Rate-dependency of residual shear strength of soils: implications for landslide evolution. Géotechnique Letters **13**(2), 105–112 (2023)

[24] Scaringi, G., Loche, M.: Temperature and rate effects on the residual shear strength of clays: a state of the art. In: Proceedings of the 6th Regional Symposium on Landslides in the Adriatic-Balkan Region, ReSyLAB2024, Belgrade, Serbia 15–18th May 2024, vol. 6, pp. 247–251 (2024). https://doi.org/10.18485/resylab.2024.6.ch37

[25] Suzuki, M., Umezaki, T., Kawakami, H., Gakkai, D.: Residual strength of soil by direct shear test. Japan Society of Civil Engineers **2000** (2000)

[26] Mitchell, J.K.: Temperature effects on the engineering properties and behavior of soils, pp. 9–28 (1969). https://onlinepubs.trb.org/Onlinepubs/sr/sr103/103-002.pdf

[27] Bucher, F.: Die restscherfestigkeit natürlicher böden, ihre einflussgrössen und beziehungen als ergebnis experimenteller untersuchungen. PhD thesis, ETH Zurich (1975)

[28] Saffer, D.M., Frye, K.M., Marone, C., Mair, K.: Laboratory results indicating complex and potentially unstable frictional behavior of smectite clay. Geophysical Research Letters **28**, 2297–2300 (2001). https://doi.org/10.1029/2001GL012869

[29] Saffer, D.M., Marone, C.: Comparison of smectite-and illite-rich gouge frictional properties: application to the updip limit of the seismogenic zone along subduction megathrusts. Earth and Planetary Science Letters **215**, 219–235 (2003). https://doi.org/10.1016/S0012-821X(03)00424-2

[30] Villar, M.V., Lloret, A.: Influence of temperature on the hydro-mechanical behaviour of a compacted bentonite. Applied clay science **26**(1-4), 337–350 (2004)

[31] Amatya, B., Soga, K., Bourne-Webb, P., Amis, T., Laloui, L.: Thermo-mechanical behaviour of energy piles. Géotechnique **62**(6), 503–519 (2012)

[32] Sun, H., Mašín, D., Najser, J., Scaringi, G.: Water retention of a bentonite for deep geological radioactive waste repositories: High-temperature experiments and thermodynamic modeling. Engineering geology **269**, 105549 (2020)

[33] Laloui, L.: Thermo-mechanical behaviour of soils. Revue Française de Génie Civil **5**, 809–843 (2001). https://doi.org/10.1080/12795119.2001.9692328

[34] Paaswell, R.E.: Temperature effects on clay soil consolidation. Journal of the Soil Mechanics and Foundations Division **93**(3), 9–22 (1967)

[35] Fredlund, D.G., Rahardjo, H.: Soil Mechanics for Unsaturated Soils. John Wiley and Sons, Canada (1993)

[36] Burghignoli, A., Desideri, A., Miliziano, S.: A laboratory study on the thermomechanical behaviour of clayey soils. Canadian Geotechnical Journal **37**(4), 764–780 (2000)

[37] Cekerevac, C., Laloui, L.: Experimental study of thermal effects on the mechanical behaviour of a clay. INTERNATIONAL JOURNAL FOR

NUMERICAL AND ANALYTICAL METHODS IN GEOMECHANICS Int. J. Numer. Anal. Meth. Geomech **28**, 209–228 (2004). https://doi.org/10.1002/nag.332

[38] Hueckel, T., Francois, B., Laloui, L.: Explaining thermal failure in saturated clays. Geotechnique **59**, 197–212 (2009). https://doi.org/10.1680/GEOT.2009.59.3.197

[39] Gens, A.: Soil-environment interactions in geotechnical engineering. Geotechnique **60**, 3–74 (2010). https://doi.org/10.1680/GEOT.9.P.109

[40] Masri, M., Sibai, M., Shao, J.-F., Mainguy, M.: Experimental investigation of the effect of temperature on the mechanical behavior of tournemire shale. International Journal of Rock Mechanics and Mining Sciences **70**, 185–191 (2014)

[41] Ng, C.W.W., Mu, Q.Y., Zhou, C.: Article effects of soil structure on the shear behaviour of an unsaturated loess at different suctions and temperatures. Can. Geotech J. **54** (2017). https://doi.org/10.1139/cgj-2016-0272

[42] Liu, H., Liu, H., Xiao, Y., McCartney, J.S.: Effects of temperature on the shear strength of saturated sand. Soils and Foundations **58**(6), 1326–1338 (2018)

[43] He, S.-H., Shan, H.-F., Xia, T.-D., Liu, Z.-J., Ding, Z., Xia, F.: The effect of temperature on the drained shear behavior of calcareous sand. Acta Geotechnica **16**, 613–633 (2021). https://doi.org/10.1007/s11440-020-01030-7

[44] Shibasaki, T., Matsuura, S., Hasegawa, Y.: Temperature-dependent residual shear strength characteristics of smectite-bearing landslide soils. Journal of Geophysical Research: Solid Earth **122**, 1449–1469 (2017). https://doi.org/10.1002/2016JB013241

[45] Liu, G., Tong, F., Tian, B., Tian, W.: Influence of atmospheric temperature on shallow slope stability. Environmental Earth Sciences **78**, 1–9 (2019)

[46] Di Maio, C., Scaringi, G., Vassallo, R.: Residual strength and creep behaviour on the slip surface of specimens of a landslide in marine origin clay shales: influence of pore fluid composition. Landslides **12**, 657–667 (2015). https://doi.org/10.1007/s10346-014-0511-z

[47] Pontolillo, D.M., De Rosa, J., Scaringi, G., Di Maio, C.: Clay creep and displacements: influence of pore fluid composition. Procedia Engineering **158**, 69–74 (2016)

[48] Shibasaki, T., Matsuura, S., Okamoto, T.: Experimental evidence for shallow, slow-moving landslides activated by a decrease in ground temperature. Geophysical Research Letters **43**, 6975–6984 (2016). https://doi.org/10.1002/2016GL069604

[49] Palazzi, E., Mortarini, L., Terzago, S., Hardenberg, J.V.: Elevation-dependent warming in global climate model simulations at high spatial resolution **52**, 2685–2702 (2019). https://doi.org/10.1007/s00382-018-4287-z

[50] Loche, M., Scaringi, G., Yunus, A.P., Catani, F., Tanyaş, H., Frodella, W., Fan, X., Lombardo, L.: Surface temperature controls the pattern of post-earthquake landslide activity. Scientific reports **12**(1), 988 (2022)

[51] Bikash, S., Steiner, J.F., Shrestha, A.B., Maharjan, A., Nepal, S., Shrestha, M.S., Bajracharya, B., Rasul, G., Shrestha, M., Jackson, M., Gupta, N.: The Melamchi flood disaster-cascading hazard and the need for multihazard risk management (2021). https://doi.org/10.53055/ICIMOD.981. https://lib.icimod.org/record/35284

[52] Adhikari, T.R., Baniya, B., Tang, Q., Talchabhadel, R., Gouli, M.R., Budhathoki, B.R., Awasthi, R.P.: Evaluation of post extreme floods in high mountain region: A case study of the melamchi flood 2021 at the koshi river basin in nepal. Natural Hazards Research **3**, 437–446 (2023). https://doi.org/10.1016/J.NHRES.2023.07.001

[53] Muñoz-Torrero Manchado, A., Allen, S., Ballesteros-Canovas, J.A., Dhakal, A., Dhital, M.R., Stoffel, M.: Three decades of landslide activity in western nepal: new insights into trends and climate drivers. Landslides **18**, 2001–2015 (2021)

[54] Shrestha, S., Shrestha, M., Babel, M.S.: Modelling the potential impacts of climate change on hydrology and water resources in the indrawati river basin, nepal. Environmental Earth Sciences **75**, 280 (2016). https://doi.org/10.1007/s12665-015-5150-8

[55] ISO3310-2: Test Sieves-Technical Requirements and Testing-Part2: Test Sieves of Perforated Metel Plate (2013)

[56] ADB: Mapping Hazards in Nepal's Melamchi River: Catchment to Enhance Kathmandu's Water Security (2021)

[57] Harris, W., White, G.N.: X-ray Diffraction Techniques for Soil Mineral Identification, vol. 5, pp. 81–115. John Wiley and Sons, Ltd, USA (2015). https://doi.org/10.2136/SSSABOOKSER5.5.C4. https://onlinelibrary.wiley.com/doi/full/10.2136/sssabookser5.5.c4

[58] Controls: TORSHEAR Ems: Automatic Ring Shear Testing Machine for Residual Strength of Soils (2023). www.controls-group.com

[59] ASTM6467: Standard Test Method for Torsional Ring Shear Test to Determine Drained Residual Shear Strength of Fine-Grained Soils. https://www.astm.org/d6467-21e01.html

[60] Scaringi, G., Di Maio, C.: Influence of displacement rate on residual shear strength of clays. Procedia Earth and Planetary Science **16**, 137–145 (2016). https://doi.org/10.1016/j.proeps.2016.10.015. The Fourth Italian Workshop on Landslides

[61] Samarakoon, R.A., Kreitzer, I.L., McCartney, J.S.: Impact of initial effective stress on the thermo-mechanical behavior of normally consolidated clay. Geomechanics for Energy and the Environment **32**, 100407 (2022). https://doi.org/10.1016/j.gete.2022.100407